Pseudopotential band structure of indium nitride

C. P. Foley* and T. L. Tansley

*School of Mathematics and Physics, Macquarie University,
North Ryde, New South Wales 2113, Australia*

The band structure, density of states, and the imaginary part of the dielectric function have been calculated for indium nitride by a pseudopotential method. Comparison with published reflectance data permits the identification of principal optical transitions at the Γ, M, K, and H symmetry points and we have been able to correct previous transition assignments. The calculated long-wavelength refractive index of 2.88 ± 0.5 compares well with experiment. The material has a direct energy gap at the zone center and the spherically symmetric extrema are well described by scalar effective masses of $0.17m_0$, $0.5m_0$ (holes), and $0.12m_0$ (electrons).

I. INTRODUCTION

Indium nitride, a hexagonal III-V compound semiconductor, has received little attention in the literature and only recently have samples with low electron concentrations and high mobilities been reported.[1] As far as we are aware, no calculated band-structure data have been published and the only report of ultraviolet reflectivity[2] available has relied on earlier calculations for gallium nitride[3] for the assignment of principal optical transitions.

Bearing in mind the band-structure similarities between the more familiar III-V compounds (the phosphides, arsenides, and antimonides of aluminium, gallium, and indium), it has been predicted[2] that similar trends will be apparent in the nitride series. This prediction is borne out by the band schemes of aluminium and gallium nitrides,[3] and here we complete the series by presenting the results of a pseudopotential calculation for indium nitride.

II. CALCULATION METHOD

Although the orthogonalized-plane-wave (OPW) method is preferable in some respects, the ease with which empirical pseudopotential calculations can be carried out and the relative success of this method when applied to other III-V compound semiconductors,[3,4] makes it the obvious choice.

The first estimates of the form factors of InN were obtained from two sources. The form factors of indium, $V_{In}(K)$, were taken from those summarized by Cohen and Heine[5] which we normalized for the appropriate lattice constant and structure.

The form factors of nitrogen were synthesized from the form factors of AlN and GaN as suggested by Bloom,[3]

$$\Omega_N V_N(K) = \Omega_{XN}[V_{XN}^S(K) - V_{XN}^A(K)] \ , \tag{1}$$

where $X = $ Ga or Al. The symmetric and antisymmetric form factors of InN are then constructed from $V_N(K)$ and $V_{In}(K)$ by

$$V_{InN}^S(K) = \Omega_{In} V_{In}(K) + \Omega_N V_N(K) \tag{2}$$

and

$$V_{InN}^A(K) = \left[\frac{\Omega_{In}}{\Omega_{InN}}\right] V_{In}(K) - V_{InN}^S(K) \ . \tag{3}$$

Here the volumes per atom are $\Omega_{In} = 175.3$ and $\Omega_{InN} = 103.6$ a.u.

The form factors of InN calculated from (2) and (3) were used as a first approximation. The experimental energy difference chosen for the final fitting, $\Gamma_6 - \Gamma_1 = 2$ eV, was achieved by varying $V_{InN}^{S,A}$ (Refs. 6 and 7). The final form factors are plotted in Fig. 1 as a function of the square of the reciprocal lattice vector. See also Table I.

The eigenvalues and eigenvectors were obtained from the Hamiltonian after augmenting the matrix with perturbation terms. We used 70 plane waves to form the basis with about 220 more plane waves being added in as perturbation terms, as described by Brust.[6] The cutoff energies chosen were $E_1 = 0.74$ Ry and $E_2 = 1.99$ Ry, giving a convergence error of less than 15 mRy.

The final form factors were used to compute the density of states and the imaginary part of the dielectric function, $\epsilon_2(\omega)$, using the Gilet-Raubenheimer integration scheme[8]
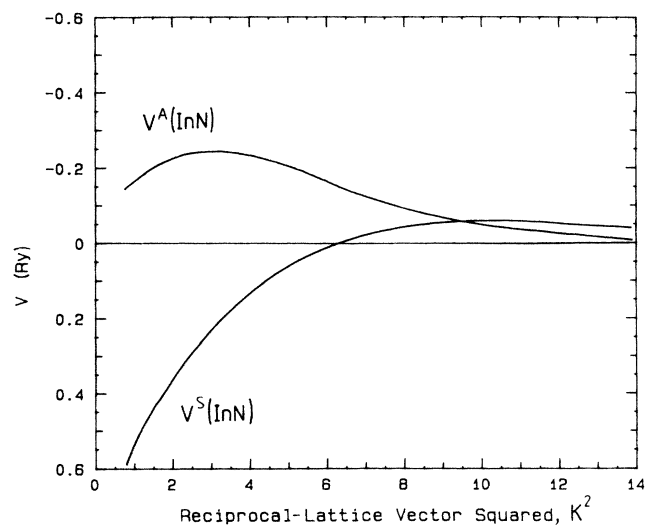

FIG. 1. Pseudopotential form factors for wurtzite InN (Rydberg units) as a function of the square of the reciprocal-lattice vector,

$$K^2 = \frac{1}{u}h^2 + \frac{1}{u}k^2 + 2\left[\frac{a_0}{c_0}\right]l^2 \ ,$$

where u is the ideal wurtzite parameter and a_0, c_0 are the lattice parameters.

TABLE I. Symmetric and antisymmetric form factors for indium nitride at values of $|K|^2$ appropriate to the wurtzite structure, extracted from the data presented in Fig. 1.

$\lvert K \rvert^2$	$V^s_{InN}(K)$ (Ry)	$V^A_{InN}(K)$ (Ry)
0	$\cdots$	$\cdots$
$\frac{3}{4}$	-0.540	$+0.141$
$2\frac{2}{3}$	-0.250	$+0.248$
3	-0.212	$+0.248$
$3\frac{4}{12}$	-0.179	$+0.248$
$5\frac{2}{3}$	-0.026	$+0.163$
$6\frac{3}{4}$	$+0.015$	$+0.080$
8	$+0.042$	$+0.060$
$8\frac{3}{4}$	$+0.045$	$+0.050$
$9\frac{5}{12}$	$+0.050$	$+0.0325$
$10\frac{2}{3}$	$+0.054$	$+0.029$
11	$+0.055$	$+0.025$
$11\frac{5}{12}$	$+0.053$	$+0.0225$
12	$+0.042$	$+0.075$
$13\frac{2}{3}$	$+0.035$	$+0.005$
$14\frac{2}{3}$	$\cdots$	$\cdots$
$14\frac{3}{4}$	$\cdots$	$\cdots$

with 144 points in a representative $\frac{1}{24}$ segment of the hexagonal Brillouin zone. In order to develop a reasonable way of handling $|M_{n,s}(K)|^2$, we computed the matrix elements for $n = 4$, $s = 5$ and $n = 4$, $s = 6$ for $\omega \geq 16$ eV as suggested by Brust.[6]

III. RESULTS AND DISCUSSION

Our calculated band structure, density-of-states function, and reflectivity spectra for polarizations parallel and normal to the c axis are shown in Figs. 2–4, respectively. Experimental reflectivity[2] data are included in Fig. 4 for comparison.

The band structure (Fig. 2) exhibits a direct band gap with the conduction- and valence-band extrema located at the center of the zone. Below the valence-band maximum at Γ are maxima at A, M, and H. Although the valence band is somewhat less flat than GaN (Ref. 8), there are close similarities as predicted.

The calculated density of states (Fig. 3) shows that the valence-band width is 9.6 eV, with a single maximum at 2.1 eV and a doublet at 6.45 and 7.05 eV. The conduction band shows maxima at 4.2, 6.8, and 8.5 eV. Unfortunately, there are at present no ultraviolet or x-ray photoemission measurements available to verify these values experimentally.

There is good agreement between experimental and calculated reflectivity peak energies and shapes although the predicted absolute magnitude is greater than observed. This difference is common in such comparisons (see, for example, Refs. 4 and 9) presumably because of surface roughness, exacerbated in this case by the polycrystalline nature of the films used.

The long-wavelength index of refraction for perpendicular polarization is calculated from our theoretical imaginary part of the dielectric function by[9]

$$n_{ir}(0) = \frac{1 + R^{1/2}(0)}{1 - R^{1/2}(0)} , \qquad (4)$$

where $R(0)$ is the high-energy reflectivity. The range of experimental values, $2.9 \pm 10\%$ (Ref. 10) and $3.05 \pm 0.1\%$ (Ref. 11), embraces our calculated value of 2.88 ± 0.15.

Considering the reflectivity spectra in more detail, we see that the fundamental gap is well understood and has been attributed to $(\Gamma_6, \Gamma_1) \rightarrow \Gamma_1$ transitions with Γ_6 calculated to be 0.2 eV above Γ_1. Spin-orbit coupling, which has been
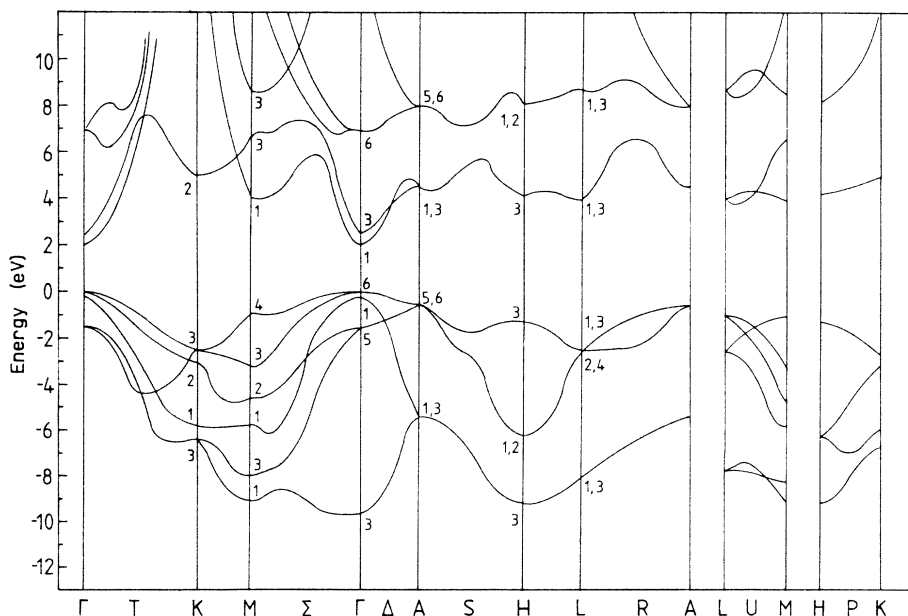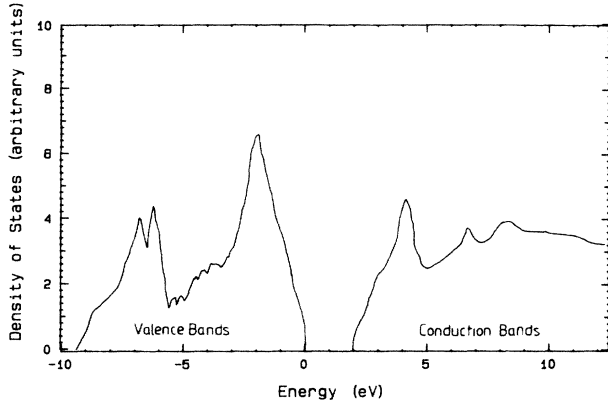

FIG. 2. The energy bands of indium nitride.

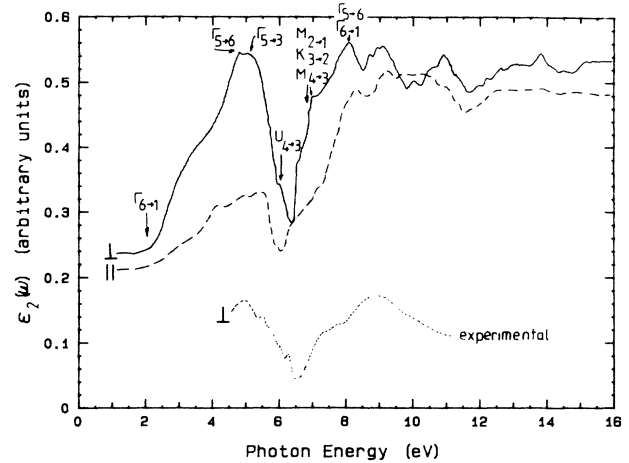FIG. 3. The calculated density of states of indium nitride.

FIG. 4. The imaginary part of the dielectric constant as a function of photon energy. Full line, perpendicular calculated; dot-dash line, parallel calculated; broken line, perpendicular experimental (from Ref. 2).

neglected in these calculations because of the lightness of the constituent elements,[9] slightly modifies the optical structure here. There are no available measurements of crystal-field splitting to give an indication of the relative positions of Γ_6 and Γ_1 in the valence bands. Nevertheless, comparison of the crystal-field-splitting measurements of GaN with its calculated band structure[9] indicated a good agreement, and suggests that InN should also display a similar behavior with $E\Gamma_6 > E\Gamma_1$, as seen in our calculated band structures.

Comparison of the reflectivity spectra of InN with other wurtzite materials (such as ZnS[4] and GaN[9]) indicates the similarity of InN to this family, and suggests that corresponding peak assignments can be made. In doing this, we disagree with the assignments made by Sobolev, Kroitu, Andreeva, and Malakhov,[2] which were based on those of GaN[3] without any reference to the specific features of InN. The fact that their spectrum was measured only to 4.5 eV could indicate their initial assignment of $\Gamma_5 - \Gamma_3$ to be incorrect.

These authors' measurements were also performed on polycrystalline thin films with the attendant possibility that the microstructure may relax the selection rules and allow parallel transitions to weakly appear in a perpendicular mea-

surement (and vice versa), as well as reducing the overall magnitude. Polarization dependence measurements on high-quality cleaved surfaces would improve these experimental results although there seems to be negligible likelihood of suitable samples of InN becoming available in the foreseeable future.

Details of the determination of each critical-point type throughout K space is given for wurtzite ZnS by Bergstresser and Cohen.[4] Table II lists the calculated critical-point energies, reflectivity peaks, and our new peak assignments for InN. Because a relatively coarse mesh was used for these calculations, we expect that the position of the peaks might be in error by up to ± 0.2 eV. Considering the mesh size, the excellent agreement between the reflectance and $\epsilon_2(\omega)$ is probably fortuitous.

Approximate effective masses for InN, obtained from the curvatures of the parabolic band extrema at $K = 0$, are $m_e^* = 0.12 m_0$, $m_h^{*\text{heavy}} = 0.5 m_0$, and $m_h^{*\text{light}} = 0.17 m_0$.

TABLE II. Identification of optical structures of wurtzite InN. Column 1 lists the important regions of the zone and column 2 lists the principal transitions in these regions. Column 3 lists the critical point (CP) energy, and column 4 lists the energy of the structures in the calculated $\epsilon_2(\omega)$ spectrum caused by the regions listed in column 1. Column 5 lists the new transition assignments for the experimental reflectivity. Column 6 lists the polarization obtained from the dipole matrix element (ME).

Region	Transition[a]	E (eV)	$\epsilon_2(\omega)$ (eV)	Expt. (eV)	ME
M_0 CP at	Γ_6-Γ_1	2	2	2(1.89)[b]	$\perp$
M_0 CP at	Γ_1-Γ_1	2.2	2	$\cdots$	$\parallel$
M_2 CP at	Γ_5-Γ_3	4	4	4.7	$\perp$
M_1 CP at	U_4-U_3	5.9	4.8		$\perp$
M_1 CP at	U_3-U_3	5.9	4.8		$\parallel$
M_2 CP at	M_2-M_1	5	5.1	4.95	$\perp$
M_2 CP at	K_3-K_2	7.5		7.2	$\perp$
Region around	H_3-H_3	5.4	5.6	5.4	$\parallel$
Region around	K_2-K_2	8.1	6.5		$\parallel$
Large region around	Γ_5-Γ_6	8.4	8.1	8.9	$\perp$
Very large region	Γ_1-Γ_1	11.4	7.35		$\parallel$

[a]Labeling of states is after Bouckaert, Smoluchowski, and Wigner (Ref. 13).
[b]See Ref. 7.

A perturbation treatment of valence- and conduction-band edge extrema[6] suggests that the electron effective mass should be inversely proportional to the band gap for a direct-gap material. For many direct-gap materials, this relationship is given by $m_e^* E_g / m_0 = 0.017$ eV (Ref. 12). This gives $m_e^* = 0.12 m_e$, in accordance with both our calculated value and the measured high electron mobilities in high-purity samples.

IV. SUMMARY

The band structure of indium nitride shows a predictable similarity to those of aluminium and gallium nitrides, as well as the other III-V compound semiconductors. The direct band gap of the nitrides is retained, while conduction- and valence-band density-of-states maxima each occur at about 2 eV from the respective extrema. Good agreement is found between published reflectivity data and the calculated dielectric function and we have been able to correct the assignment of peaks in these spectra. Since the band extrema are parabolic it is appropriate to describe free carriers in terms of scalar effective masses of $0.5 m_0$ and $0.17 m_0$ for heavy and light holes, respectively, and $0.12 m_0$ for electrons. The light electron is responsible for the relatively high mobility reported in n-type material.

ACKNOWLEDGMENTS

*Present address: CSIRO Division of Applied Physics, National Measurement Laboratory, Commonwealth Scientific and Industrial Research Organization, P.O. Box 218, Lindfield, New South Wales 2070, Australia.

[1]T. L. Tansley and C. P. Foley, Electron. Lett. 20, 1066 (1984).

[2]V. V. Sobolev, S. G. Kroitu, A. F. Andreeva, and V. Ya. Malakhov, Fiz. Tekh. Poluprovodn. 13, 823 (1979) [Sov. Phys. Semicond. 13, 485 (1979)].

[3]S. Bloom, J. Phys. Chem. Solids 32, 2027 (1971).

[4]T. K. Bergstresser and M. L. Cohen, Phys. Rev. 164, 1069 (1967).

[5]M. L. Cohen and V. Heine, Solid State Phys. 24, 208 (1970).

[6]D. Burst, Phys. Rev. 134, A1337 (1964).

[7]Our recent measurements on samples with a variety of electron concentrations indicate a room-temperature value of 1.89 eV in the low-concentration limit, and that a substantial Moss-Burstien shift for $n > 10^{18}$ cm^{-3} is probably responsible for the frequently quoted figure of 2.0 eV used here.

[8]G. Gilet and L. J. Raubenheimer, Phys. Rev. 144, 390 (1966).

[9]S. Bloom, G. Harbeke, E. Meier, and I. B. Ortenburger, Phys. Status Solidi B 66, 161 (1974).

[10]J. Misek and F. Srobar, Elektrotech. Cas. 30, 690 (1979).

[11]M. Ilegems, J. Cryst. Growth 13/14, 360 (1972).

[12]C. Kittel, Introduction to Solid State Physics, 5th ed. (Wiley, New York, 1976), p. 224.

[13]L. P. Bouckaert, R. Smoluchowski, and E. Wigner, Phys. Rev. 50, 58 (1936).